X-RAY TOMOGRAPHIC CONTROL STATION FOR WELD JOINTS OF FES FOR POWER REACTORS

A. Aleksandrov[1], Yu. Zhukov[1], Yu. Karlov[1], V. Rozhkov[1], S. Chatschin[1], Yu. Obidin[2], A. Potashnikov[2], Yu. Chuguy[2].
[1] JSC Novosibirsk Chemical Concentrates Plant, Russia, Novosibirsk; [2] Design Technological Institute for Scientific Instrument Engineering, Siberian Branch of Russian Academy of Sciences, Russia, Novosibirsk

Abstract: Brief description of automatic X-ray tomographic control station for weld joints of rod-type FEs is given in this work. Algorithms for obtaining multi-layer panoramic tomograms are described. Results of automatic detection and measurement of defects such as pores are set forth. The suggested solutions make it possible to perform full control of a weld for one minute, to detect and measure in automatic mode pores of 100 μm and over with error not exceeding 15%.
Key words: computed tomography, defect, non-destructive assay, detection, measurement, processing, image reconstruction.

1. Introduction: Safety of nuclear power plants to a considerable extent is provided by highly reliable operation of fuel assemblies (FAs) and their components. Therefore the quality of fuel element (FE) fabrication during their industrial production is controlled according to many indices [1]. One of quality indices is reliability of weld joints. Due to all said above there is a necessity to improve old means and to create new highly efficient means of weld automatic control. X-ray computed tomography (XCT) applies to new highly efficient methods of non-destructive assay as it provides high sensitivity to local inhomogeneities. Tomography provides the possibility to study fine internal structure of items that increases trustworthiness of control especially vital for nuclear power plants.
In literature [2-5] considerable attention is put to research of tomography accuracy and sensitivity as applied to control of manufactured articles, certification and checkup of tomographs, as well as to issues related to the increase of equipment capacity and degree of its automation. One of tomography urgent goals – automatic detection and measurement of minor defects in FEs welds during their production. As far as we know this problem is not yet solved at the present time.
Authors studied the above mentioned problem using highly efficient X-ray station for tomographic control of FEs [6] as applied to detection and measurement of pores up to 300 μm.

2. Tomograph description: Object of control is a zirconium tube of 9.1 mm in diameter, which is welded up by plugs at both ends (Figure 1). Area of control has a cylindrical form of 2 mm high.

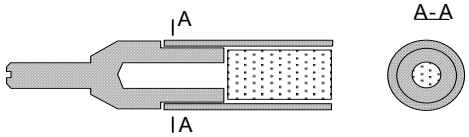

Figure 1. *View of FE with lower plug*

Typical defects are air-bubble voids of 100μm and more in diameter, aggregations of small pores, local cracks and poor penetration.
Full processing cycle of one item (FE with zirconium cladding) including time of loading, registration of projection data, detection of defects and rejection took one minute. Detection of defects and determination of their dimensions were performed using panoramic images of weld.

Panoramic images of FE weld joints were obtained by means of X-ray tomographic station that is designed for operation in workshop conditions. Composition and structure of X-ray tomographic station are showed in Figure 2.

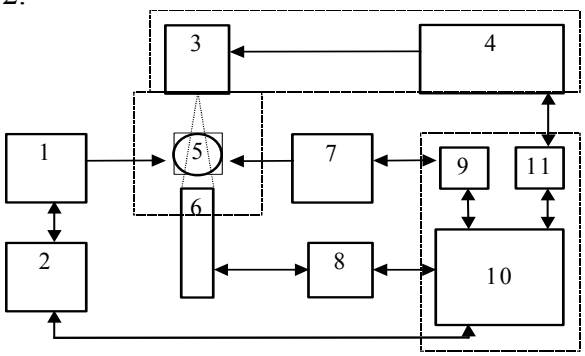

Figure 2. *Structure of tomographic station (1 – transporting table, 2 – table controller, 3 – X-ray tube, 4 – X-ray unit, 5 - FE, 6 – detector unit, 7 – scanning unit, 8 – video camera adapter, 9 – scanning system controller, 10 - computer, 11 – control module)*

Registration channel comprises an X-ray tube, collimators and a detector unit. Collimators form a conical beam covering the whole area of control at any aspect. Shadowgraph is registered by matrix detector.

Software is operated by Windows 98 operation system. Standard graphic formats of TIFF and BMP data representation are used for image storage. Basic operation mode of station in production line – automatic. Software has a developed interactive mode. Communication between program components is performed only via data flows that made it possible to create open software and to switch on extra functions or procedures easily.

Maximum detection ability of X-ray computed tomography (even if there is no unit noise) is limited by quantum Poisson noise of X-rays. The following relation can be used to determine minimal volume of reliably detected defects [10]:

$$V_д = \xi_V \, |C_д|^{-1} \, \alpha_t^{1/2} \, D_э^{-1/2} \, k_м^{-1} . \qquad (1)$$

Where $V_д$ - minimal volume of reliably detected local defect, ξ_V – proportionality factor, $C_{ä} = (\mu_{ô} - \mu_{ä}) / \mu_{ô}$ - contrast of linear attenuation factor (LAF) of defect and background, α_t – width of controlled layer, $D_э$ – exposure dose, $k_м$ – limit of spatial resolution, $\mu_д$ - linear attenuation factor of defect, $\mu_ф$ - linear attenuation factor of background.

Thus minimal volume of defects detected by XCT methods is directly proportional to square root of controlled layer width and inversely proportional to limit of spatial resolution, contrast of defect linear attenuation factor and square root of exposure dose.

It is evident from formula (1) that to increase the detection ability it is necessary to increase the contrast of linear attenuation factor, exposure dose and spatial resolution. As a result of quantum noise and dependence of material linear attenuation factor on radiant energy $\mu(E)$, there is an optimal radiant energy (E_0) when informativity of projection data is maximal. When energy of X-ray photons $E<E_0$ is insufficient, accuracy of projection data is extremely decreased. In its turn at unjustifiably high energy $E>E_0$ the decrease of linear attenuation factor contrast is not compensated by the increase of projection data accuracy, as well as the informativity of X-ray computed tomography is also decreased but more smoothly than during the deviation to lower-energy region. It is known [11], that for majority of industrial structures the optimal energy is reached when the product of average thickness l and linear attenuation factor $\mu(E_0)$ of controlled object material $\overline{\mu(E_0)l} = 2...4$. In connection with insufficient

reference data on zirconium theoretically we calculated the dependence of zirconium linear attenuation factor and contrast range of 0.001mm^3 defect on photon energy.

Dependence of zirconium linear attenuation factor on radiant energy was calculated on the ground that linear attenuation factor of material is proportional to cube of radiation wavelength: $\mu(\lambda) = \alpha\lambda^3 + \beta$, where $\lambda = hc/E$ - wavelength; h – Planck constant; c – velocity of light. Parameters α and β were defined more accurately by means of experimentally obtained absorption values for different radiant energy.

Curves of these dependencies are showed in Figure 3 and Figure 4. Measured values of linear attenuation factor are marked by signs in Figure 3.

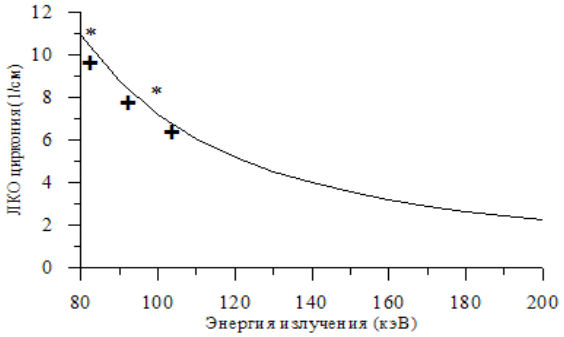

Figure 3. *Dependence of zirconium linear attenuation factor on radiant energy*

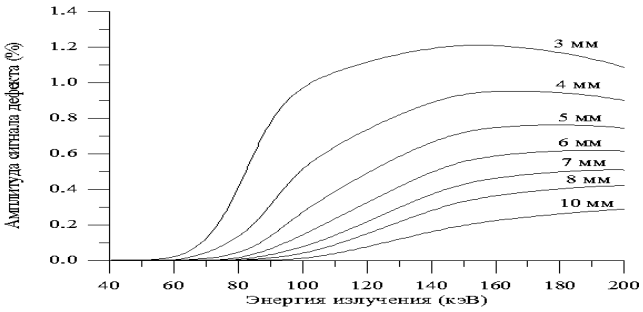

Figure 4. *Dependence of relative amplitude of 100 μm defect on radiant energy and zirconium thickness*

Performed theoretical analysis showed that to detect defects of 100 μm and less in control objects made of zirconium up to 10 mm thick it is necessary to have X-ray energy of 160 -180 keV.

3. Reconstruction algorithms: As controlled item has an axial symmetry and small thickness of layer with defects, the reconstructed function can be represented as a sum: $f(x,y,z) = f_0(x,y,z) + g(x,y,z)$, where $f_0(x,y,z)$ - known distribution of linear attenuation factor in non-defective item; $g(x,y,z)$ - distribution of linear attenuation factor in thin cylindrical layer containing defects. Consideration of a priori information about control object made it possible to develop algorithms of panoramic reconstruction that reconstruct structure of cylindrical layer at lesser number of calculations [7].

Comparison of developed algorithms was made according to visual quality of images, noise level, reconstruction time, reliability of automatic defect detection after threshold processing.

Reconstruction of radius panorama ρ using weighted projections and providing accurate reconstruction of thin layer for objects with axial symmetry was made in accordance with the following formula:

$$Q_\rho(m,j) = \frac{1}{K}\sum_{k=0}^{K-1} p_k[\rho\cos(\frac{2\pi n}{M} - \frac{2\pi k}{K}), j]\,|\sin(\frac{2\pi n}{M} - \frac{2\pi k}{K})| \qquad (2)$$

Hereinafter $Q_\rho(m,j)$ – reconstructed value of linear attenuation factor at panorama point with coordinates m and j; index k indicates the ordinal number of projection. Total number of projections is equal to K. Projections are registered through equal angle interval at complete revolution of item $\varphi = 2\pi$. Each projection consists of M lines ($j \in \{0,..,M-1\}$). Projection lines have length L ($i \in \{0,1,..,L-1\}$) and are oriented perpendicular to rotation axis.

Reconstruction algorithms using complete projections ($k\min = 0;\quad k\max = K-1$) or limited projections (from $k\min = \frac{2\pi}{K}\arccos(\frac{s_0}{\rho});$ to $k\max = \frac{2\pi}{K}\arccos(\frac{L-s_0}{\rho})$) were applied as standard algorithms in accordance with formula (3):

$$Q_\rho(m,j) = \frac{1}{k\max - k\min + 1} \times \sum_{k=k\min}^{k\max} \tilde{p}_k[\rho\cos(\frac{2\pi m}{M} - \frac{2\pi k}{K}), j] \qquad (3)$$

In formulas (2) and (3) non-filtered projection is specified as $p_k(i,j)$, and filtered projection - as $\tilde{p}_k(i,j)$. Radius of reconstructed layer ρ is given in pixels. Rotation axis on the projection has the coordinate s_0. Radius and position of axis have real values for accurate calculations.

Examples of reconstructed panoramas according to the above-mentioned algorithms are represented in Figures 5 and 6. In Figure 5 there are panoramic images reconstructed using complete filtered projections for three different values of radius. On the first panorama (Figure 5a) there is an image of internal layer where minor deep item defects are well seen. In the external layer (Figure 5c) on the contrary there are no fine pores. All defects are visible on the image (Figure 5b) reconstructed for the mean radius and the amplitude is sufficient for their automatic detection. This makes it possible to reconstruct only one layer during control process.

In Figure 6 there are images of the same layers but reconstructed using weighted projections. Reconstruction is performed 5 times faster using method of weighted projections the than using complete filtered projections. Images are of satisfactory quality.

Comparison of images (Figures 5, 6) shows that in each individual case it is possible to find the balance between quality and reconstruction time.

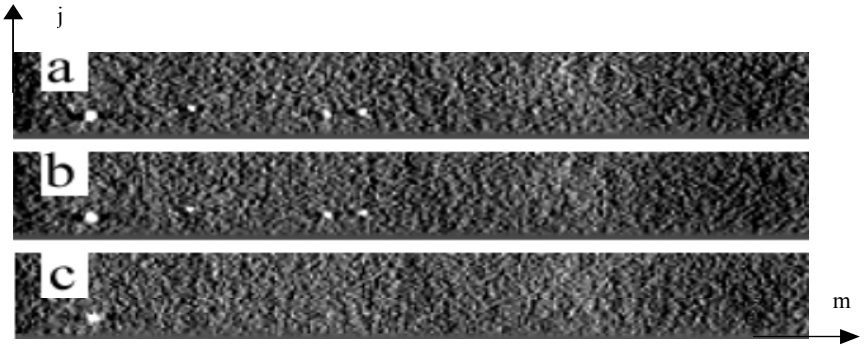

Figure 5. *Panoramic images of three cylindrical layers reconstructed using complete projections (a - radius ρ=3.8 mm; b - ρ=4.2 mm; c - ρ=4.5 mm).*

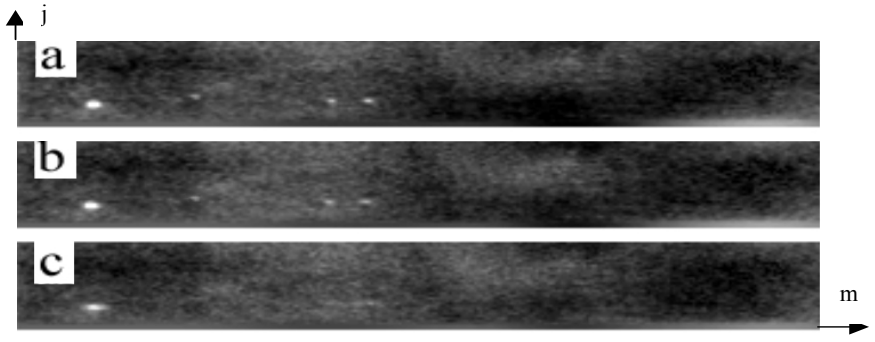

Figure 6. *Panoramic images of layers showed in Figure 5 and reconstructed using weighted projections*

4. Detection and measurement of defects: Let's examine the process of defect detection and measurement using tomograms. It is known [3], that distribution of linear defect attenuation factor $\mu_д(x,y,z)$ reconstructed by tomograph is a convolution of initial distribution $\mu_д(x,y,z)$ with point scattering function (PSF) $h(x,y,z)$:

$$\mu_д(x,y,z) = \iiint \mu_д(\xi,\eta,\gamma) \times h(x-\xi, y-\eta, z-\gamma) d\xi d\eta d\gamma \qquad (4.1)$$

For geometrical structures of small volume (at dimensions comparable with dimensions of point scattering function) their form and dimensions on reconstructed image are substantially deformed and are determined by form and dimensions of scattering function. Useful consequence of model (4.1) is an interrelation of defect geometrical dimensions and tomogram amplitude parameters in neighborhood with dimensions about point scattering function that makes it possible to determine defect volume according to luminance of their images. For example, for defects such as air-bubble voids it can be considered that $\mu_д(x,y,z) = const$. In this case it is easy to show that integral of reconstructed distribution of linear attenuation factor $\mu_д(x,y,z)$ is proportional to product of initial defect volume $V_д$ by volume of point scattering function $V_{фрт}$:

$$\iiint \mu_д(x,y,z) dx dy dz = \alpha V_д V_{ðð} \qquad (4.2)$$

Passing to discrete representations the integral can be changed by a sum B_Σ of all elements of reconstructed 3D defect. In this case after have measured on tomograms luminances B of all points belonging to defect, it is possible to determine its volume $V_{д.}$

$$V_д = \frac{1}{\alpha V_{ðð}} \sum_i (B_i - \overline{B}_ô) = k B_\Sigma, \qquad (4.3)$$

where k – proportionality factor; $\overline{B}_ф$ – average value of background luminance.

Calculation of total luminance is easy to perform in two steps: firstly tomograms of different cross-sections containing defects are added together and then all points of defect are found and added together on the total image. In case of panoramic reconstruction the thickness of reconstructed layer can be controlled, for example, by using limited projections. In case when the thickness of reconstructed layer exceeds linear dimensions of defect, defect luminance on tomogram occurs to be integrated by coordinate perpendicular to the layer, therefore it is enough to sum up luminances on the image of one layer passing through the defect.

In Figure 7 there is a tomogram fragment of 18×18 elements with image of actual 250 μm defect. Semi-transparent plane corresponds to threshold $P=B_ф+4\sigma$.

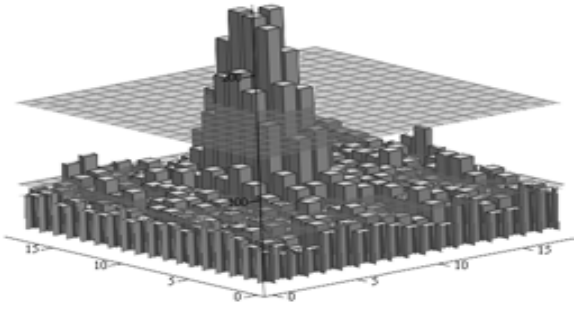

Figure 7. *Image of defect having 250 μm in diameter*

In the given example the total luminance of pixels exceeding the threshold is lower than the complete luminance because defect points lower than threshold but higher than background level are not taken

into account. It is evident that the smaller defect the bigger the possibility of mistake concerning the determination of its luminance.

During studies the procedure for determination of defect dimensions comparable with dimensions of point scattering function, which is based on measurement of total luminance, was developed. The peculiarity of measurement procedure consists in the use of information about form of defect image and its coordinates that makes it possible to increase the accuracy of dimensions determination. Defect coordinates are determined in the step of detection by subprogram (or operator) and are known before measurement. Form of minor defect images on tomogram is considered to be close to form of transfer characteristic. This characteristic is approximated by gaussoid with sufficient accuracy $K(\mathrm{f}) = \exp(-\frac{\mathrm{f}^2}{8})$, where f – spatial frequency (1/mm). It corresponds to transfer characteristic (scattering function) of the following type:

$$h(x, y, z) = \exp(-\frac{x^2 + y^2 + z^2}{r^2}) \tag{4.4}$$

At experimentally found value $r \approx 0.11$ mm, volume of tomograph point scattering function is $\approx 8 \times 10^{-3}$ mm^3, that corresponds to volume of cube with edge 0.2 mm or sphere having 0.25 mm in diameter.

Assuming that form of reconstructed defect is invariable an optimal detector can be used. In case of noise with normal distribution it consists of a filter which is matched with form of signal and threshold device [8]. Nucleus of matched filter is calculated in accordance with the formula (4.4) of scattering function.

All points of image whose luminance exceeds the specified threshold P are considered to be defects. Separate points are considered as one defect if they are located inside the circle with radius r. Center of defect is its center of mass calculated using the filtered image in the local vicinity of each of points exceeding the threshold. Besides centers of masses calculated for points related to the same defect virtually coincide that makes it possible to exclude the repeated detection of defects.

On tomogram points of defect are located around the center in the circle with radius r. Specifying the level L, above which, for example, there are 90% of all defect luminance energy:

$$L = \int_{-r}^{r} \exp(-\frac{r^2}{0{,}0128})\, dr = 0{,}9\,; \tag{4.5}$$

it is possible to find the radius r of reconstructed defect according to Sheppard tables. During summing up of luminances around center of defect in circle with radius r, it can be stated that the obtained value of luminance will be 90% of complete luminance. This luminance value is corrected up to 100% and used for the determination of true defect diameter.

Luminances of defect points are added together and background level is determined during one passage in local neighborhood (19×19) of defect center using initial (non-filtered) image. In this case pixels of image local region situated in the circle of radius r are considered to belong to the defect and all others – to the background. Background "substitution" equal to the product of average background by defect area is subtracted from the sum of luminances of defect elements. Value obtained this way is considered to be total luminance of defect (B_Σ).

If it is accepted that the defect has spherical form (form of pores the most frequently found), defect luminance (proportional to volume) and its diameter $\boldsymbol{D}$ are linked by power law:

$$D = \alpha\, B_\Sigma^{1/3}\,, \tag{4.6}$$

where $\alpha = \sqrt[3]{12/k\pi}$.

So to determine linear dimensions of defects using their tomograms it is sufficient to know total luminance and proportionality factor α.

5. Results of experimental studies: Experimental check of the developed procedure was performed to determine its accuracy and limits of applicability. Obtained results are represented as diagrams and tables. In experiments FEs with artificial defects were used. Those artificial defects were obtained by drilling holes in polished section of weld.

Artificial defects were measured by low-coherent interferometry using the unit described in [9]. In Figure 8 there is an image of one of artificial defects obtained by using interferometric unit. Diameter of defect is 160 μm, its depth - 180 μm.

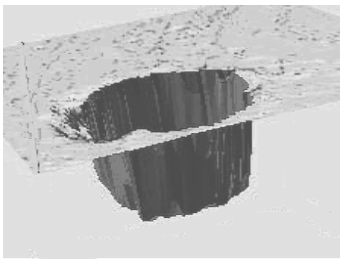

Figure 8. *View of defect (diameter - 160 μm, depth - 180 μm)*

Panoramic tomograms of fabricated specimens were used during studies. Experimentally obtained dependence of pore diameter on luminance is showed in Figure 9.

This dependence is well approximated by transfer function $D_{\text{äåô}} = 13{,}6 * B_{\Sigma}^{0,4}$. Roof-mean-square deviation of measured parameters from gauge function is 12.1 μm, maximum – 29.5 μm. Relative error of defect diameter determination using gauge function does not exceed ±8% (standard deviation of relative error on all studied defects – 4.5%)

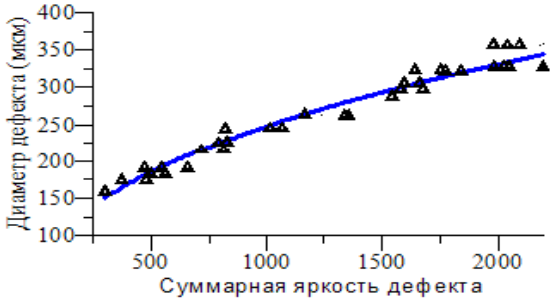

Figure 9. *Dependence of defect dimension on luminance*

In Table 1 there are measured luminances for internal pores of two rejected FEs. During X-ray testing of these items pore dimensions were estimated as 200, 300 and 350 μm respectively. Defect dimension was determined using gauge function given in Figure 9.

Table 1

No. points	No. of item	Radius of panorama							Luminance B_{Σ}	Defect dimension (μm)
		72	74	76	78	80	82	84		
1	9161051	854	**991**	914	874	802	-	-	991	215
2	9956066-1	1967	2195	3021	**3403**	3346	2926	2625	3403	320
3	9956066-2	2103	2354	2888	3532	**3652**	3341	3191	3652	330

Radius of panorama is given in pixels (pixel is equal to 50 μm). Maximum luminance, which is obtained during the passage of reconstructed layer through the defect, is printed in thick type. Change of defect luminance during change of radius of reconstructed layer makes it possible to determine the defect level depth.
Thus a good correspondence between the chosen model and experimental results is obtained.

6. Conclusion: Problem of automatic detection and measurement of defects such as pores in FE weld during fabrication by tomographic method is solved.
Algorithm of panoramic reconstruction using weighted projections is suggested and realized in X -ray tomographic station. Such algorithm makes it possible to reduce reconstruction time 5 times without considerable loss of reconstructed image quality.

Taking into account form of tomograph transfer characteristic during matched filtering reduces more than 2 times the volume of reliably detected minor defects (diameter up to 130 μm) and increases determination accuracy of their coordinates.

Developed procedure makes it possible to determine in automatic mode pore dimensions within the range from 130 to 300 μm with error not exceeding 15% of linear dimension.

Obtained results prove that multi-layer panoramic tomography can be efficiently used in detecting and measuring of defects such as pores in weld joints of tubular and axially symmetrical manufactured articles.

7. Literature:

1. A.S. Shtan. Automated quality control during FE fabrication for NPP. Devices and control systems, 1995, No.11, p.12-13
2. E. I Wineberg, I.A Kazak, V.P. Kurozaev. Reproduction accuracy of controlled object spatial structure in X-ray industrial tomography. Flaw detection 1980 No. 10, p.5-14
3. E. I Wineberg, V. I. Goncharov, I.A Kazak, V.P. Kurozaev. Sensitivity of X-ray computed tomography during control of industrial items with local defects. Flaw detection, 1980 No. 10, p.14-20
4. E. I Wineberg, I.A Kazak, V.P. Kurozaev, G. Z. Plotkina. Materials and certification method of standard specimens for checkup of X-ray computed tomographs. Flaw detection, 1982 No.9, p.7-14
5. N. R. Kuzelev, V. N. Tutubalin, L. S. Salakatova. Accuracy characteristics of radiation computed tomography during control of rod-type FEs. Flaw detection, 1987, No.7, p.50
6. V. V. Vorobyev, Yu. K. Karlov, Yu.V. Obidin, A.K. Potashnikov, E. V. Sysoyev, I. G. Chapaev. "X-ray tomographic control station for weld joints of FEs ". Detectors and systems, 1999 No.2
7. V.P. Kosykh, Yu.V. Obidin, A.K. Potashnikov. Comparative analysis of reconstruction algorithm for the fuel element tomographic control station. Pattern Recognition and Image Processing, Vol9, ¹1, 1999, pp.145-147.
8. 8.N.S. Shestov. Extraction of optical signals on the background of random disturbances.- M.,1967, 347 p.
8. I. V. Golubev, E. V. Sysoyev, Yu. V. Chuguy. Measurement of surface defects on the basis of low-coherent interferometry. Detectors and systems. 1999, No.6, p.25-29
9. Non-destructive assay and diagnostics. Reference book edited by V. V. Kluyev, Moscow, "Machine-building", 1995.
10. X-ray technics. Reference book in two volumes, edited by V. V. Kluyev, Moscow, " Machine-building", 1992.